Journal of Electroanalytical Chemistry, 377 (1994) 163–175

Copper-zeolite-modified electrodes: An intrazeolite ion transport mechanism

Jian-wei Li and Gion Calzaferri*

Institute for Inorganic and Physical Chemistry, University of Berne, Freiestrasse 3, CH-3000 Berne 9 (Switzerland)

(Received 17 December 1993; in revised form 21 March 1994)

Abstract

A new method for preparing mechanically stable dense 1 μm zeolite monograin layers on substrate electrodes allows detailed information on the electrochemical behaviour of Cu^{2+}-zeolite-modified electrodes to be obtained. The conductivity of the Cu^{2+}-Y-zeolite layers depends on the electrolyte cations and decreases in the order $Cs^+ > K^+ > Na^+ > Li^+$. Experiments on thick zeolite layers composed of stacked zeolite particles show that only the Cu^{2+} ions in the first layer take part in the electrode process. Significant differences between the cyclic voltammograms of Cu^{2+} at the unmodified glassy carbon electrodes and at the zeolite-modified electrodes are observed. Our experiments clearly demonstrate that the electrochemical processes at monograin Cu^{2+}-Y-zeolite-modified electrodes are of intrazeolite ion transport type. Cu^{2+} ions in A zeolites are electrochemically 'silent' in the potential range from 0.5 to -0.8 V/SCE, in strong contrast with Cu^{2+}-Y-zeolite but in agreement with the fact that A zeolites do not support high Cu^{2+} exchange.

1. Introduction

Modification of electrodes with zeolites has evoked considerable interest. Reviews of zeolite-modified electrodes and electrode-modified zeolites and of their analytical applications have recently been published [1,2]. Possible uses of such electrodes have been discussed in a review of the materials science aspects of zeolites [3]. Current research is driven by the desire to impart zeolitic properties to the electrodes. Therefore in a successful modification the charge, size and shape selectivity of the zeolite should be imparted to the electrode.

Several techniques have been used in the preparation of zeolite-modified electrodes. Two of them are very common. A simple approach is to cast an electrode coating from a suspension of zeolite particles and a dissolved polymer. After evaporation of the solvent, the polymer enfolds the zeolite and holds it to the surface of a substrate electrode such as platinum, glassy carbon or SnO_2 conducting glass to form a porous layer [4–8]. The second method relies on pressing the powder mixture into electrode grids. It has been used for the preparation of zeolite-modified electrodes with different composites [4,9–13]. We have developed a simple method for producing dense zeolite monograin layers on substrate electrodes and we have shown that the preparations thus obtained are well suited to electrochemical experiments [14].

Several studies of copper-zeolite-modified electrodes have been reported and two mechanisms to describe their electrochemical behaviour have been proposed, one intrazeolitic and the other extrazeolitic [7,8,15,16]. However, the experiments reported so far are not conclusive because in all cases the layers of the zeolite-modified electrodes were too thick to be suitable for obtaining mechanistic information. We shall see that the two mechanisms suggested so far in the literature are not sufficient to describe the observations made by us. It has been found to be necessary to distinguish between an intrazeolite electron transport mechanism and an intrazeolite ion transport mechanism [14,17]. We shall show that an intrazeolite ion transport mechanism is appropriate for describing the electrochemical behaviour of Cu^{2+}-Y-zeolite-modified electrodes, whereas in zeolite A the Cu^{2+} ions are electrochemically 'silent'.

* To whom correspondence should be addressed.

0022-0728/94/$7.00
SSDI 0022-0728(94)03455-L

2. Experimental

2.1. Chemicals and apparatus

A zeolite (Linde 4A, Baylith T, Bayer) and Y zeolite (LZY-52, Union Carbide) were used as received. All chemicals were analytical grade and were used without further purification. Double-distilled water was used in all experiments. Electrochemical experiments were carried out in a standard one-compartment three-electrode cell with a water jacket for connection to a thermostatic water circulator. The counterelectrode was a Pt sheet electrode. The reference electrode was a saturated calomel electrode (SCE). The potentials were referred to this electrode (SCE) and not corrected for *IR* drop and liquid junction potentials. Voltammetric experiments were performed with an EG&G model 273 potentiostat and model 270 electrochemical analysis system.

2.2. Preparation of zeolite samples

Samples with different degrees of Cu^{2+} exchange were prepared by the following procedure: 100 ml of a dispersion containing 1.00 g of zeolite and the appropriate amount of $CuCl_2 \cdot H_2O$ was stirred for 24 h at room temperature (about 20°C) then filtered and washed with double-distilled water until no Cl^- ions could be detected using $AgNO_3$ in the filtrate. Finally, the Cu^{2+}-exchanged zeolite was dried for 24 h at 60°C. The Cu^{2+}-exchanged zeolite samples prepared in this way were preconditioned in atmosphere at room temperature for 48 h before they were used and analyzed.

These Cu^{2+}-exchanged zeolite samples are denoted as Cu_xNa_{12-2x}-A and Cu_xNa_{56-2x}-Y, where x is the degree of Cu^{2+} exchange. They were analysed by CIBA-GEIGY AG. The combined analytical data are expressed as unit cell compositions in Table 1.

2.3. Electrode preparation

Glassy carbon disc electrodes (diameter 3 mm) with Teflon sheathing were used as substrate electrodes. Before coating with zeolite, they were pretreated in the following way. They were washed first ultrasonically in 0.1 M HNO_3 for 5 min and then thoroughly with water. After this they were polished to a mirror finish under rotation at 3000 rev min^{-1} with 0.3 μm Al_2O_3, washed ultrasonically in water three times and stored in a clean area ready for modification with zeolite.

A dispersion containing 60.0 mg of zeolite and 15.00 ml of water in a vial with a polyethylene stopper was prepared by shaking vigorously and dispersing ultrasonically for about 1 h. It was repeatedly used as a mother dispersion. Before use, it was shaken and dispersed in an ultrasonic bath for at least 1 h, and after use it was stoppered and sealed with parafilm to prevent evaporation of water. With a micropipette, 5 μl of this dispersion was carefully applied to the surface of the pretreated glassy carbon electrode and allowed to dry very slowly in a covered beaker at room temperature for about 10 h.

A micropipette was used to drop 5 μl of polystyrene solution (0.75 mg of polystyrene in 20 ml of tetrahydrofuran) onto the dried zeolite layer; this solution was then evaporated at room temperature. The coatings obtained contained 20 μg of zeolite and ca.0.2 μg of polystyrene.

2.4. Procedure for the voltammetric experiments

Supporting electrolyte solution (40 ml) was added to the cell. The solution was purged with Ar for at least 20 min before starting the measurements. The voltammetry measurements were carried out immediately after immersion of the electrode into the electrolyte solution at 20°C. The surface of the electrolyte solution was protected by Ar during the measurements. Electrolyte solutions were adjusted to pH 6.0 with 0.1 M HCl or 0.1 M MOH ($M = Li^+$, Na^+, K^+, Cs^+) under Ar bubbling.

3. Results and discussion

3.1. Structure of the zeolite layers

In order to analyse the layer structure of the zeolite-modified electrodes, scanning electron microscopy (SEM) was performed for the zeolite layers

TABLE 1. Zeolite analysis

Zeolite	Unit cell composition	Cu^{2+} exchange degree/%
Na-A	$Na_{12}(AlO_2)_{12}(SiO_2)_{12} \cdot 7.64H_2O$	0
Na-Y	$Na_{56}(AlO_2)_{56}(SiO_2)_{142} \cdot 244H_2O$	0
$Cu_{0.05}Na_{11.9}$-A	$Cu_{0.05}Na_{11.9}(AlO_2)_{12}(SiO_2)_{12} \cdot 24H_2O$	0.9
$Cu_{0.10}Na_{11.8}$-A	$Cu_{0.10}Na_{11.8}(AlO_2)_{12}(SiO_2)_{12} \cdot 24H_2O$	1.7
$Cu_{0.15}Na_{11.7}$-A	$Cu_{0.15}Na_{11.7}(AlO_2)_{12}(SiO_2)_{12} \cdot 24H_2O$	2.6
$Cu_{0.22}Na_{11.6}$-A	$Cu_{0.22}Na_{11.6}(AlO_2)_{12}(SiO_2)_{12} \cdot 24H_2O$	3.6
$Cu_{0.28}Na_{11.4}$-A	$Cu_{0.28}Na_{11.4}(AlO_2)_{12}(SiO_2)_{12} \cdot 25H_2O$	4.7
$Cu_{0.57}Na_{10.9}$-A	$Cu_{0.57}Na_{10.9}(AlO_2)_{12}(SiO_2)_{12} \cdot 27H_2O$	9.6
$Cu_{10.6}Na_{34.8}$-Y	$Cu_{10.6}Na_{34.8}(AlO_2)_{56}(SiO_2)_{142} \cdot 257H_2O$	37.7

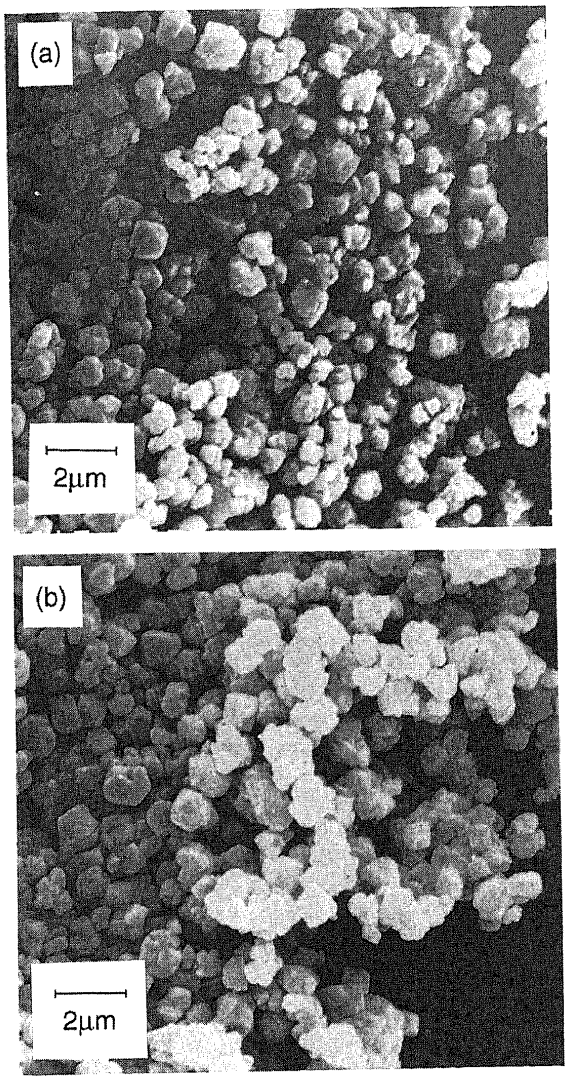

Fig. 1. Scanning electron micrographs of $Cu_{10.6}Na_{34.8}$-Y layers on the surface of glassy carbon disc electrodes: (a) without polystyrene binder; (b) with polystyrene binder.

with and without polystyrene binder. A typical result is shown in Fig. 1. The uncoated parts in the right-hand side represent the surface of the glassy carbon electrode, where the zeolite coatings were carefully peeled off before performing SEM in order to give a clear view of the thickness of the zeolite layer. Figure 1 shows that the coating achieved by our procedure consists of one to two condensed monograin layers of zeolite particles of average size about 1 μm^3 and that the thickness of the zeolite layer is about 1 μm. The structure of the zeolite layer prepared by this method is completely different from that reported by other authors [6,7]. In their procedures, thick porous zeolite + polymer layers are obtained and the zeolite particles are embedded in the polystyrene film.

Comparison of Figs. 1(a) and 1(b) shows that no obvious polystyrene layers are present in Fig. 1(b) but these two kinds of coatings show a significant difference in mechanical stability. The mechanical stability of the zeolite coatings without polystyrene binder is very low and the polystyrene binder improves it substantially. For example, the coatings without polystyrene binder are easily removed from the surface of the glassy carbon electrode when they are immersed in a slowly stirred solution, but no apparent loss of zeolite from the surface of the glassy carbon electrode in aqueous solution has been observed for the coatings with polystyrene binder even under rotation at 3000 rev min^{-1}. This indicates that the polystyrene binder produces a remarkable increase in the mechanical stability of the zeolite coatings on the surface of the glassy carbon electrode.

3.2. *Mechanical stability and reproducibility*

The mechanical stability of the zeolite-modified layer on the surface of a substrate electrode is crucial for the reproducibility of the experiments. In general, poor mechanical stability of zeolite layers decreases the experimental reproducibility and a good experimental reproducibility indicates that the mechanical stability of the zeolite layers is high. This was tested with nine $Cu_{10.6}Na_{34.8}$-Y modified electrodes by performing cyclic voltammetry in 0.1 M NaCl aqueous solution at a scan rate of 20 mV s^{-1}. The resulting cyclic voltammograms show two reduction peaks (A and B) and two oxidation peaks (C and D), which are illustrated in Fig. 2 and will be discussed later. The peak current and the charge under peak A are listed in Table 2. They show good

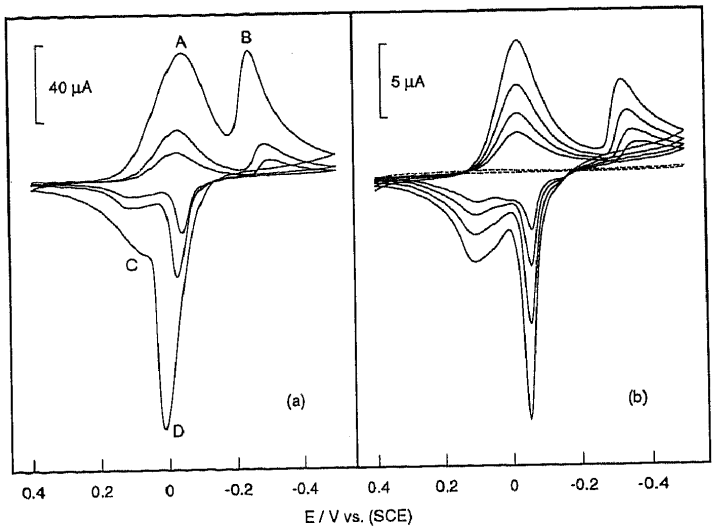

Fig. 2. Cyclic voltammograms of a $Cu_{10.6}Na_{34.8}$-Y-modified electrode in 0.1 M NaCl aqueous solution at pH 6, 20°C, a scan rate of 20 mV s^{-1}, an initial potential of 0.4 V and a switching potential of −0.5 V: (a) cycles 1–3; (b) cycles 4–7. The broken curve is the baseline obtained from a Na-Y-modified electrode under the same conditions.

TABLE 2. Reproducibility test [a]

	Experimental values									m	SD
$I_{cp(A)}/\mu A$	64.5	68.4	62.4	65.7	68.3	65.6	63.5	67.0	65.3	65.6	2.03
$Q_{(A)}/\mu C$ [b]	635	677	615	646	677	649	625	663	645	648	21.6

[a] The experimental values were obtained from nine different $Cu_{10.6}Na_{34.8}$-Y-modified electrodes: m, mean; SD, standard deviation; $I_{cp(A)}$, peak current of cathodic peak A; $Q_{(A)}$, charge under the peak A.
[b] The charge was obtained by integrating the area under the peak A.

reproducibility which indicates that the zeolite layer on the glassy carbon prepared by our procedure is mechanically stable. We conclude that this kind of zeolite-modified glassy carbon electrode is well suited to electrochemical studies.

3.3. *Influence of the location of Cu^{2+} in zeolites on voltammetric behaviour*

Figure 3 shows some crystallographically identified cation positions of zeolites A and Y. In zeolite A, site SII is at the centre of a six-ring face with sites SII′ and SII* displaced into and out of the β-cage along the triad axis respectively, while site SIII is adjacent to the four-ring face in the α-cage. Site SV, which is not indicated in Fig. 3, is at the centre of the octagonal window. In zeolite Y, site SI is at the centre of the hexagonal prism and site SI′ is displaced towards the ß-cage from the hexagonal prism. Sites SII, SII′ and SII* are defined in the same way as in the case of zeolite A. In fully hydrated zeolite Na-A, a six-fold coordinated Cu^{2+} complex bound to three water molecules and three oxygen atoms of the zeolite framework is located at site SII′ in the β-cage, while in fully hydrated zeolite Y, Cu^{2+} ions are located only in the supercage coordinated to six water molecules to form $[Cu(H_2O)_6]^{2+}$ ions which can rotate freely [18,19].

The cyclic voltammograms of the $Cu_{10.6}Na_{34.8}$-Y-modified electrode in Fig. 2 show two reduction peaks and two oxidation peaks in the scan range from 0.4 to −0.5 V/SCE. When an Na-Y-modified electrode is scanned under identical conditions, no peaks are observed, as is shown in Fig. 2(b). Peaks A and B in the voltammogram of the $Cu_{10.6}Na_{34.8}$-Y-modified electrode are clearly due to the electrochemical reduction of Cu^{2+} and Cu^{+} ions, and peaks C and D correspond to the electrochemical oxidation of reduced Cu^{+} and Cu^{0}.

The charging current of the baseline is very small compared with the faradaic current. Assuming that the charging current is the same for the $Cu_{10.6}Na_{34.8}$-Y- and the Na-Y-modified electrodes, the charge passed in the first cathodic peak A ($Q_{(A)} = 648\ \mu C$) can be estimated directly by integrating the area under the peak A. The amount of $Cu_{10.6}Na_{34.8}$-Y zeolite used for the modified electrode was 20 μg, which therefore contained a total of 1.2×10^{-8} mol of Cu^{2+} ions. About 56% of Cu^{2+} ions were electrochemically reduced to Cu^{+} at this scan rate in 0.1 M NaCl aqueous solution. This indicates that the bulk Cu^{2+} ions are electrochemically reduced during the negative scan since the external surface area of the zeolite crystals is about 1% of the total equivalent surface area [20].

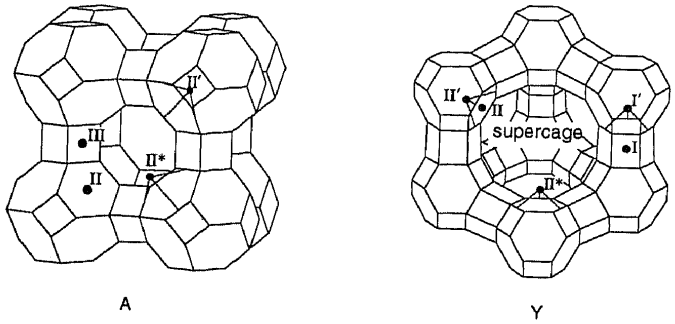

Fig. 3. Structures of zeolites A and Y showing crystallographically identified cation positions.

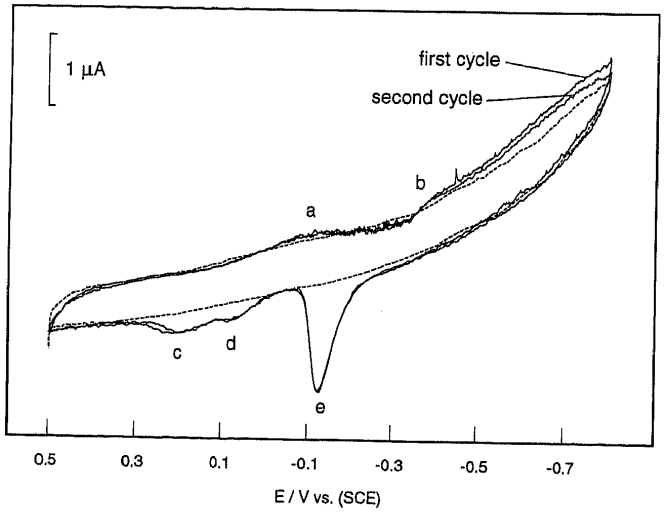

Fig. 4. Cyclic voltammograms of a $Cu_{0.22}Na_{11.6}$-A modified electrode in 0.1 M NaCl aqueous solution at pH 6, 20°C and a scan rate of 20 mV s^{-1}. The initial potential is 0.5 V and the switching potential is −0.8 V. The broken curve is the baseline obtained from a Na-A-modified electrode under the same conditions.

The same experiments were carried out with Cu^{2+}-A-modified electrodes of varying degrees of Cu^{2+} exchange for which completely different behaviour was observed. A typical cyclic voltammogram is shown in Fig. 4. In comparison with the voltammogram of the Na-A modified electrode, only two very small cathodic peaks and three anodic peaks appear, which are denoted as a, b, c, d and e respectively. The peak currents are almost the same for all degrees of Cu^{2+} exchange (0.9% to 9.6%). Not more than 0.5% to 1% of the Cu^{2+} ions in zeolite A are electrochemically reduced. This indicates that the Cu^{2+} ions in zeolite A are electrochemically 'silent' in the potential range from 0.5 to −0.8 V/SCE. The very small currents observed may result from the reduction of Cu^{2+} ions adsorbed on the surface of zeolite A and/or leached out by ion exchange. The difference between the voltammetric behaviour of Cu^{2+}-A- and Cu^{2+}-Y-modified electrodes seems to be due to the different coordination and mobility of Cu^{2+} ions in zeolites A and Y.

In comparison with Cu^{2+} ions in zeolite Y, it can be expected that diffusion of Cu^{2+} ions in zeolite A is much slower owing to their coordination to the zeolite framework, the smaller cages and channels, and the slow migration of Cu^{2+} ions from the β- to the α-cages. It seems that this hindered transport is consistent with the very small current in Fig. 4. This agrees with the fact that zeolite A does not support more than about 6% of Cu^{2+}. At higher loadings corrugation of the crystals is observed and very high loading results in complete destruction of the zeolite framework [21]. The coordination of Cu^{2+} can be described in terms of distinct rigid polyhedra, while the alkali cations exhibit less well defined and less rigid coordination polyhedra. Therefore it seems that strain is induced in the zeolite framework upon exchange of the alkali ions by Cu^{2+}. This strain increases with increasing exchange level until the framework ruptures. The looser framework of zeolites X and Y can compensate better for this strain than the more compact zeolite A [21].

The oxidizability of a metal ion complex decreases with increasing stability constant. In the case of Cu^{2+} ions in zeolite A, the coordination to the zeolite framework may result in a decrease of their oxidizability of Cu^{2+} such that they cannot be reduced in the potential range from 0.5 to −0.8 V/SCE. In the following, we focus on the voltammetric behaviour of the Cu^{2+}-Y-modified electrodes which do not show the complications of Cu^{2+}-A zeolites.

3.4. *Influence of the thickness of the zeolite layer*

In order to investigate the influence of the thickness of the zeolite layer on the electrochemical response, zeolite-modified electrodes containing different amounts of zeolite $Cu_{10.6}Na_{34.8}$-Y have been prepared and voltammetry experiments have been carried out under the same conditions as shown in Fig. 2. Table 3 presents the charges passed in the first cathodic peaks in the first cycles for the electrodes containing 20, 40, 60 and 80 μg of $Cu_{10.6}Na_{34.8}$-Y respectively. As discussed above, when 20 μg of $Cu_{10.6}Na_{34.8}$-Y are coated on the glassy carbon electrode, the thickness of the coating is about 1 μm. Accordingly, the approximate thicknesses of about 2, 3 and 4 μm correspond to zeolite layers containing 40, 60 and 80 μg of $Cu_{10.6}Na_{34.8}$-Y respectively. The charge Q_A increases only slightly on increasing the amount of $Cu_{10.6}Na_{34.8}$-Y from 20 to 60 μg and remains constant for higher loading. This observation indicates that only the Cu^{2+} ions within the zeolite particles which directly contact the surface of the glassy carbon electrode (the first layer in Fig. 5) take part in the electrode process. The Cu^{2+} ions within the zeolite particles which do not directly contact the surface of the glassy carbon electrode are electrochemically 'silent' because otherwise the measured charges would be directly proportional to the amount of $Cu_{10.6}Na_{34.8}$-Y on the electrode.

TABLE 3. Influence of the thickness of the zeolite layer on the electrode response [a]

$W_z/\mu g$	20	40	60	80
$Q_A/\mu C$	648±26	692±38	704±42	706±42

[a] Voltammetry experiments were carried out with nine different electrodes under the same conditions as shown in Fig. 2: W_z, amount of zeolite $Cu_{10.6}Na_{34.8}$-Y on the surface of the glassy carbon electrode; Q_A, charge under peak A as shown in Fig. 2.

A thick zeolite layer on a substrate electrode is composed of several zeolite particle layers. According to their function in the electrode process, they can be divided into the two parts illustrated in Fig. 5. The layer in which the zeolite particles directly contact the surface of the substrate electrode is denoted the first layer and the layers in which the zeolite particles do

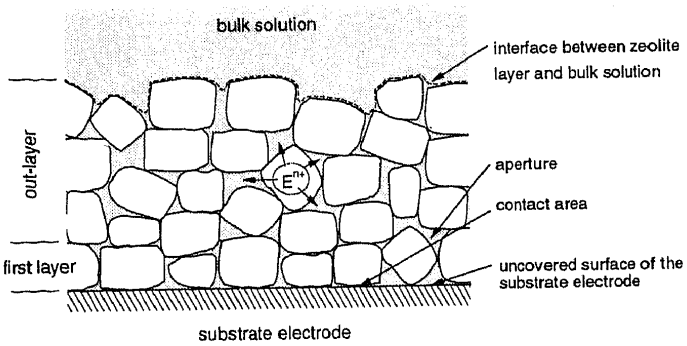

Fig. 5. Proposed arrangement of a thick zeolite layer on a substrate electrode: E^{n+}, electroactive ions.

not directly contact the surface of the substrate electrode are denoted the out-layer. The area at which the surface of the substrate electrode and the zeolite particles contact each other is called the contact area. The surface of the substrate electrode consists of the contact area and the uncovered part.

Upon insertion of an E^{n+}-exchanged zeolite-modified electrode into an electrolyte solution, the electrolyte solution will permeate the apertures between zeolite particles in the zeolite layer and ion exchange will occur at the surface of the zeolite particles. In Fig. 5, the arrows indicate the leaching of the electroactive E^{n+} ions out of the zeolite into the apertures by ion exchange. The diffusion of the leached E^{n+} ions from the apertures to the bulk solution is hindered with respect to that of the leached E^{n+} ions at the interface between the zeolite layer and the bulk solution. This means that the first layer is in an environment with a particular E^{n+} concentration. Therefore the loss of E^{n+} ions from the first zeolite layer is smaller than in the case of the monograin layer. With increasing thickness of the zeolite layer, diffusion of E^{n+} ions from the apertures to the bulk solution becomes more difficult. When it reaches a certain thickness, the concentration of the leached E^{n+} ions in the apertures no longer changes. In this case, the smallest amount of E^{n+} ions is leached out of the first layer. This is probably the main reason why the observed charges slightly increase with increasing $Cu_{10.6}Na_{34.8}$-Y from 20 to 60 μg and become constant at higher loadings.

The E^{n+} ions in the apertures of the zeolite layer also diffuse to the uncovered surface of the substrate electrode where they can undergo an electrochemical reaction. Whether this extrazeolite reaction is a main electrode process or a side-process only depends on the system. If the leaching of electroactive species out of the zeolite is fast enough within a certain experimental time-scale (i.e. at a certain scan rate in voltammetry) and if the area of the uncovered surface of the substrate electrode is larger than the contact area, it can become a main electrode process which means that an extrazeolite mechanism applies.

3.5. Ion exchange and determination of relative diffusion rates of ions within the zeolite

Ion exchange is a very important property of zeolites. In electrochemical studies of zeolite-modified electrodes, electroactive species can be concentrated within zeolites by this property. Electroactive species can also leach out of zeolites by ion exchange with electrolyte cations during the measurements. Therefore electrode processes at zeolite-modified electrodes are much influenced by ion exchange processes.

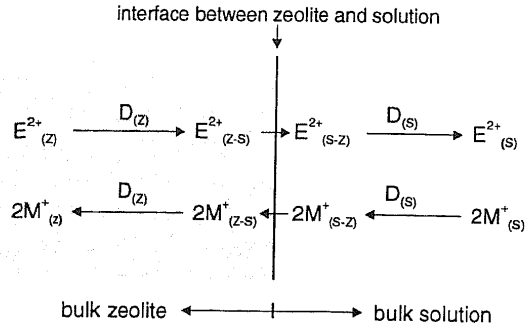

Fig. 6. Ion exchange processes occurring at the interface between zeolite and solution: E^{2+} and M^{+} are the electroactive ion and the electrolyte cation respectively; $D_{(z)}$ denotes diffusion of ions within the zeolite and $D_{(S)}$ denotes diffusion in the solution.

For simplicity, we discuss a system in which the electroactive species is a divalent cation E^{2+}, and the co-cation in the zeolite and the electrolyte cation are M^{+}. Upon insertion of the E^{2+}-exchanged zeolite-modified electrode into the electrolyte solution, ion exchange occurs between E^{2+} in the zeolite and M^{+} in the solution. This ion exchange process (Fig. 6) can be divided into three subprocesses: (1) ion exchange at the interface between the zeolite and the solution; (2) diffusion of E^{2+} and M^{+} in the cavities and channels of the zeolite; (3) diffusion of E^{2+} and M^{+} in the solution. Ions diffuse much faster in the solution than within the zeolite and the ion exchange at the zeolite|solution interface is very fast. Therefore the rate of the whole ion exchange process is controlled by the diffusion of E^{2+} or M^{+} within the zeolite [20]. In the strict sense, diffusion of E^{2+} and M^{+} within the zeolite, which is discussed here, is an apparent diffusion because the mobilities of E^{2+} and M^{+} located at different sites and in the different cages of the zeolite are different. The extent of exchange of the E^{2+} ions out of the zeolite by M^{+} depends on the nature and concentration of E^{2+} and M^{+}, the structural characteristics of the zeolite and the solvent. From the thermodynamic point of view, the amount of E^{2+} exchanged out of the zeolite into the solution depends on the selectivity coefficient. The larger the selectivity coefficient, the less E^{2+} will be exchanged out of the zeolite into the solution by M^{+}. In the actual voltammetric experiments, the volume of solution is much larger than that of the zeolite layer on the substrate electrode. Therefore, even if all the electroactive species E^{2+} originally encapsulated in the zeolite leached out into the solution, the concentration of E^{2+} in the solution would always be much smaller than that of M^{+} which is usually of the order of 0.1 M. Hence if the time of immersion of the E^{2+}-exchanged zeolite-modified electrode in the solution is long enough to reach

equilibrium, most E^{2+} ions will exchange out of the zeolite into the solution.

From the kinetic point of view, the amount of E^{2+} exchanged out of the zeolite into the solution is controlled by the rate of the ion exchange process. As we discussed above, the rate of the whole ion exchange process is controlled by the diffusion of E^{2+} or M^+ within the zeolite. Thus the amount of E^{2+} exchanged out of the zeolite into the solution is controlled by the diffusion of E^{2+} or M^+ within the zeolite.

Obviously, when the voltammetric experiments of the E^{2+}-exchanged zeolite-modified electrodes are carried out, leaching of the electroactive species E^{2+} out of the zeolite into the solution by ion exchange cannot be avoided except when the electroactive species E^{2+} is too large to escape from the zeolite cage [22,23]. In order to minimize the loss of E^{2+} ions from the zeolite during the experiments, the measurements are performed immediately after insertion of the E^{2+}-exchanged zeolite-modified electrodes into the solution.

Figure 2 shows a continuous decrease of the cathodic and anodic currents which is primarily due to the leaching of Cu^{2+} and /or Cu^+ out of the zeolite Y by ion exchange with the electrolyte cation Na^+ during the potential scan. To confirm this and to investigate the influence of the electrolyte cations on the ion exchange process, cyclic voltammetric experiments have been performed on the $Cu_{10.6}Na_{34.8}$-Y-modified electrodes after ion exchange for a certain time in a separate solution containing different alkali cations. The results of these experiments are shown in Fig. 7. Curve 5 corresponds to the first cycle in Fig. 2. Curves 1, 2, 3 and 4 are also first cycles under the same conditions but recorded after ion exchange by immersing the electrodes into 20 ml of 0.1 M CsCl (curve 1), KCl (curve 2), NaCl (curve 3) and LiCl (curve 4) aqueous solutions (without stirring) for 20 s, washing them with double-distilled water and transferring them into the 0.1 M NaCl solution in the cell. Compared with curve 5, the currents of curves 1–4 decreased in the order

$$I_{Li} > I_{Na} > I_K \gg I_{Cs} \quad (1)$$

This indicates that the rate of loss of Cu^{2+} ions of zeolite Y by ion exchange increases in the order

$$Li^+ < Na^+ < K^+ \ll Cs^+ \quad (2)$$

If the diffusion of Cu^{2+} within the Y zeolite is slower than that of all the other cations, then the ion exchange process is controlled by its diffusion within the Y zeolite and the rate of loss should be independent of the electrolyte cation. If the diffusion of Cu^{2+} within the Y zeolite is faster than that of all the other cations, then the rate of loss of Cu^{2+} depends on the

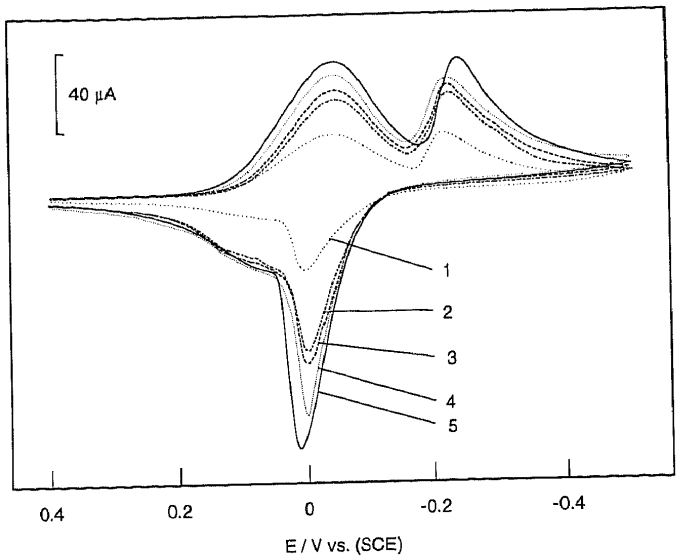

Fig. 7. Cyclic voltammograms of the $Cu_{10.6}Na_{34.8}$-Y-modified electrodes in 0.1 M NaCl aqueous solution after immersion in (1) 0.1 M CsCl, (2) KCl, (3) NaCl and (4) LiCl for 20 s. Curve 5 corresponds to the first cycle in Fig. 2. (For details see text.)

electrolyte cation. Sequence (2) clearly demonstrates that the rate of loss of Cu^{2+} of the Y zeolite depends on the electrolyte cation in the solution. Therefore it can be concluded that the order of decreasing diffusion of the tested ions within the Y zeolite is

$$Cu^{2+} \geq Cs^+ > K^+ > Na^+ > Li^+ \quad (3a)$$

or

$$Cs^+ > Cu^{2+} > K^+ > Na^+ > Li^+ \quad (3b)$$

This important finding has consequences for the mechanism of the electrochemical reactions at Cu^{2+}-Y-modified electrodes. Although the diffusion coefficients of ions in zeolites could not be obtained in this experiment, it provides us with their relative speed of diffusion within zeolites.

3.5. Voltammetric behaviour in chloride-containing electrolytes

The voltammetric behaviour of the $Cu_{10.6}Na_{34.8}$-Y-modified electrode and of Cu^{2+} ions at the unmodified glassy carbon electrode shown in Fig. 8 is significantly different. The peak potential $E_{p(A)}$ of A shifts towards negative values and the peak potential $E_{p(B)}$ of B shifts towards positive values. This indicates clearly that the electrochemical reduction of Cu^{2+} and of Cu^+ at the $Cu_{10.6}Na_{34.8}$-Y-modified glassy carbon electrode does not occur at the uncovered surface of the glassy carbon electrode following ion exchange of Cu^{2+} ions out of the Y zeolite into the solution because otherwise the $Cu_{10.6}Na_{34.8}$-Y-modified electrode and Cu^{2+} ions at the unmodified glassy carbon electrode should show

the same behaviour. However, this observation is not sufficient to decide whether the electrochemical reduction of Cu^{2+} ions at the $Cu_{10.6}Na_{34.8}$-Y-modified electrodes occurs at the contact area or in the bulk of the zeolite.

3.6. *Voltammetric behaviour in nitrate-containing electrolytes*

Figure 9(a) shows voltammograms of $Cu_{10.6}Na_{34.8}$-Y-modified electrodes and of Cu^{2+} ions at the unmodified glassy carbon electrode in 0.1 M $NaNO_3$ in the range from 0.4 to −0.6 V/SCE under the same conditions as in Fig. 8. The voltammograms for Cu^{2+} at the unmodified glassy carbon electrode show one cathodic and three anodic peaks, which we denoted as I_{GC}, II_{GC}, III_{GC} and IV_{GC} respectively. Peaks III_{GC} and IV_{GC} may be due to some complications in the electrode process. Peaks I_{GC} and II_{GC} indicate that, in the case of nitrate electrolyte, the electrochemical reduction of Cu^{2+} ions at the unmodified glassy carbon electrode occurs via a single two-electron step. The voltammogram of the $Cu_{10.6}Na_{34.8}$-Y-modified glassy carbon electrode shows two cathodic peaks and one broad anodic peak, which we denoted as I, II and III respectively. The relative heights of the peaks I and II change to some extent from one electrode to another, but both can always be observed although sometimes one of them becomes a shoulder. This may be caused by small differences between different $Cu_{10.6}Na_{34.8}$-Y-modified electrodes. The broad peak III of Fig. 9(a) may contain two unseparated peaks as shown in Fig. 9(b). We observed that the voltammetric behaviour of the $Cu_{10.6}Na_{34.8}$-Y-modified electrodes is strongly affected by the electrolyte anions. This indicates that the electrochemical reduction of Cu^{2+} ions at the $Cu_{10.6}Na_{34.8}$-Y-modified electrode does not occur within the bulk of the zeolite, otherwise the same voltammetric behaviour should be observed in both chloride and nitrate electrolytes because at this concentration the imbibition of either chloride or nitrate ions into the bulk of the zeolite is negligible due to charge restriction [24,25].

In Figs. 8 and 9 the waveforms of the voltammograms of the unmodified glassy carbon electrode shift to a positive current after the potential at which Cu^0 is produced. This is due to a change in the surface state of the unmodified glassy carbon electrode caused by deposits of Cu^0. From this, we conclude that no Cu^0 is deposited at the surface of the glassy carbon electrode in the case of the $Cu_{10.6}Na_{34.8}$-Y-modified electrodes. This explanation is supported by the voltammetric behaviour of the $Cu_{10.6}Na_{34.8}$-Y-modified electrode in 0.1 M $NaNO_3$ as a function of the switching potential as shown in Fig. 9(b). The anodic current increases when the switching potential is more positive. A possible explanation is that the Cu^0 atoms and/or clusters produced during the cathodic process migrate deeper

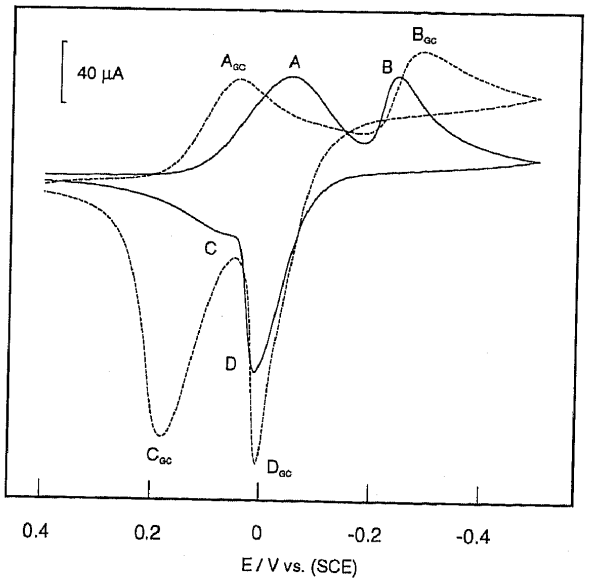

Fig. 8. Cyclic voltammograms of a $Cu_{10.6}Na_{34.8}$-Y-modified electrode in 0.1 M NaCl aqueous solution (solid curve) and of the unmodified glassy carbon electrode in 0.1 M NaCl+8.5 mM $CuCl_2$ (broken curve) at 20°C and a scan rate of 20 mV s^{-1}. The initial potential is 0.4 V and the switching potential is −0.5 V. The curves are the first cycles.

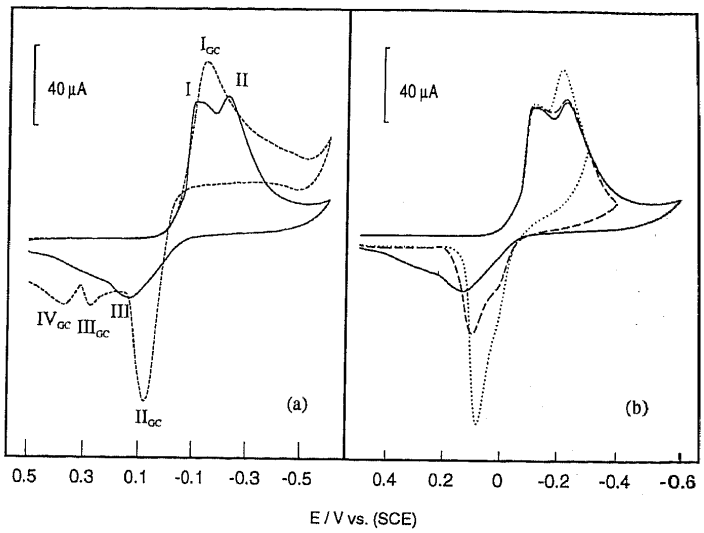

Fig. 9. (a) Cyclic voltammograms of a $Cu_{10.6}Na_{34.8}$-Y-modified electrode in 0.1 M $NaNO_3$ aqueous solution (solid curve) and of the unmodified glassy carbon electrode in 0.1 M NaCl+6.5 mM $Cu(NO_3)_2$ (broken curve) at 20°C and a scan rate of 20 mV s^{-1}. The initial potential is 0.4 V and the switching potential is −0.5 V. The curves are the first cycles. (b) Cyclic voltammograms of $Cu_{10.6}Na_{34.8}$-Y-modified electrodes in 0.1 M $NaNO_3$ aqueous solution as a function of switching potential under the same conditions as in (a). The switching potentials are −0.6, −0.4 and −0.3, respectively.

into the zeolite and some of them (i.e. those far away from the contact area) cannot be re-oxidized during the anodic process. The more positive the switching potential, the less time is available for the Cu^0 atoms and/or clusters to migrate into the zeolite; thus fewer of them are deep enough in the zeolite to be oxidized. As a result, the anodic current increases.

The voltammograms of the $Cu_{10.6}Na_{34.8}$-Y-modified electrode in 0.1 M $NaNO_3$ show two cathodic and two anodic peaks respectively, a fact that has not hitherto been reported. We can conclude that the electrochemical processes at the $Cu_{10.6}Na_{34.8}$-Y-modified glassy carbon electrode have to be interpreted by an intrazeolite ion transport mechanism.

3.7. *Influence of the electrolyte cations*

To investigate the influence of the electrolyte cations the experiments with a $Cu_{10.6}Na_{34.8}$-Y-modified electrode in 0.1 M MCl aqueous solutions have been carried out in two potential ranges, with all other conditions the same as in Fig. 8. Figure 10 shows the voltammograms in the potential range from 0.4 to −0.5 V, and Fig. 11 shows them in the potential range where only the electrochemical reduction of Cu^{2+} to Cu^+ can occur. Experiments with Cu^{2+} at the unmodified glassy carbon electrode have been carried out under the same conditions and the Cu^{2+} concentration has been adjusted in each solution to make the current at peak A_{GC} almost equal to that at peak A. The peak currents and charges observed in these voltammograms are given in Table 4, and the corresponding peak potentials, the apparent formal potentials and the peak potential differences are listed in Table 5.

Almost the same peak potentials (Table 5) are observed for Cu^{2+} ions at the unmodified glassy carbon electrode in the different electrolytes. This indicates that the voltammetric behaviour of Cu^{2+} ions at the unmodified glassy carbon electrode is not affected by

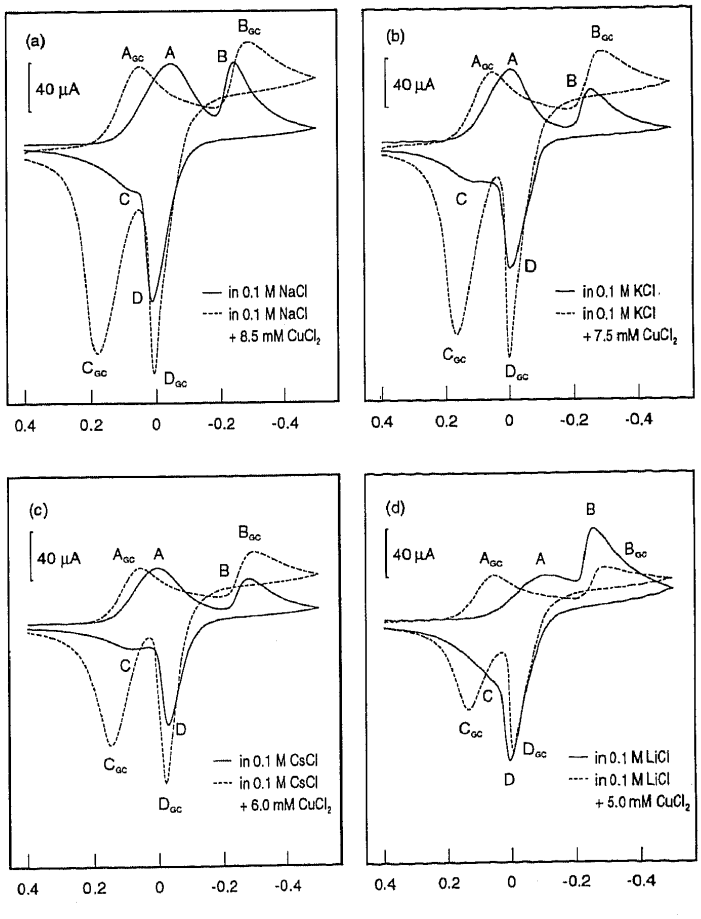

Fig. 10. Cyclic voltammetric behaviour of $Cu_{10.6}Na_{34.8}$-Y-modified electrodes (solid curve) and of Cu^{2+} ions at the unmodified glassy carbon electrode (broken curve) in different alkali chloride solutions. The other experimental conditions are the same as in Fig. 8.

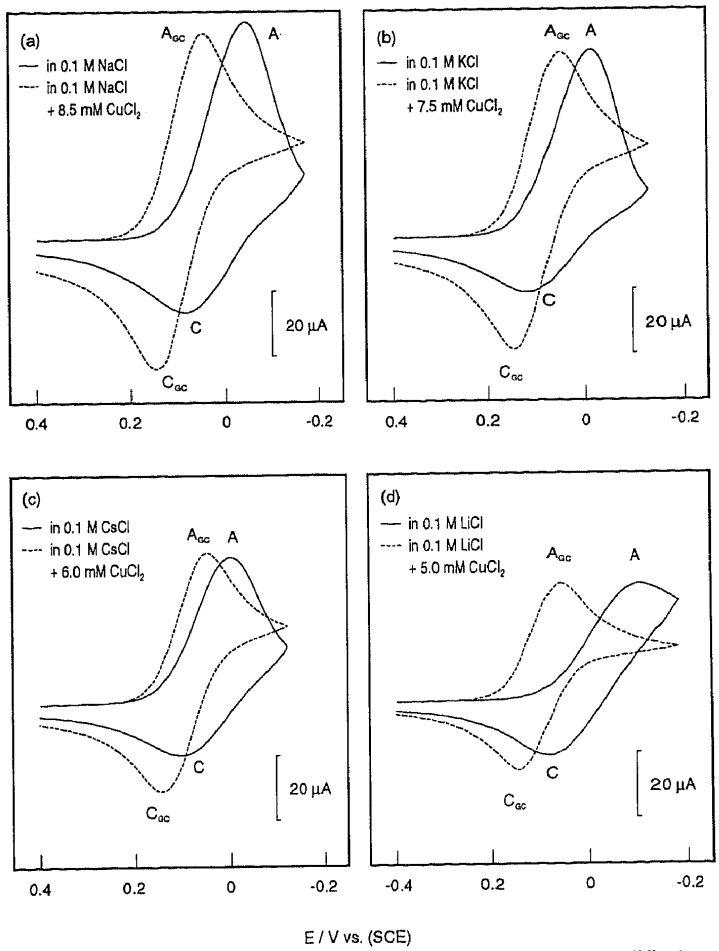

Fig. 11. Cyclic voltammetric behaviour of $Cu_{10.6}Na_{34.8}$-Y-modified electrodes (solid curve) and of Cu^{2+} ions at the unmodified glassy carbon electrode (broken curve) in different alkali chloride solutions. The switching potentials are (a) −0.17 V, (b) −0.13 V, (c) −0.12 V and (d) −0.18 V. The other experimental conditions are the same as in Fig. 8.

TABLE 4. Peak currents and charges of $Cu_{10.6}Na_{34.8}$-Y-modified electrodes in different electrolytes [a]

MCl (0.1 M)	$I_p/\mu A$			Q/mC		Q_A/Q_T [b]/%
	A	B	c	A	B	
NaCl	65.4	66.2	23.6	0.648	0.355	56
KCl	58.7	38.3	16.2	0.518	0.258	45
CsCl	45.2	30.7	20.5	0.404	0.264	35
LiCl	35.7	51.6	33.4	0.402	0.399	35

[a] The data are obtained from Figs. 10 and 11: A, B, C, D, A_{GC}, B_{GC}, C_{GC} and D_{GC} represent the peaks as shown in Figs. 10 and 11; $Q_T = nFN_T$ where N_T is the total amount of moles of Cu^{2+} ions in the zeolite layer and Q_A is the charge under peak A.

the electrolyte cations. Reversible behaviour of Cu^{2+}/Cu^+ is observed for Cu^{2+} at the unmodified glassy carbon electrode; for instance, in Fig. 11 the ratio of the anodic to the cathodic peak currents is close to unity, while in Fig. 10 the ratio of the anodic to the cathodic peak current is much greater than unity. This observation indicates that the peak C_{GC} is strongly affected by the redox process of Cu^+/Cu^0. This may be due to some complications in the electrode process caused by deposits of Cu^0 on the surface of the unmodified glassy carbon electrode. This effect is not observed in the voltammograms of the $Cu_{10.6}Na_{34.8}$-Y-modified electrodes which further indicates that the electrochemical reaction at the $Cu_{10.6}Na_{34.8}$-Y-modified electrodes is of intrazeolite character.

The voltammetric behaviour of the $Cu_{10.6}Na_{34.8}$-Y-modified electrodes in chloride electrolytes is strongly affected by the electrolyte cations. As shown in Figs. 10 and 11, the peak currents and peak potentials depend on the electrolyte cation. The potentials of peaks A and C shift towards negative values, and the potentials of peak B shift slightly towards positive values with

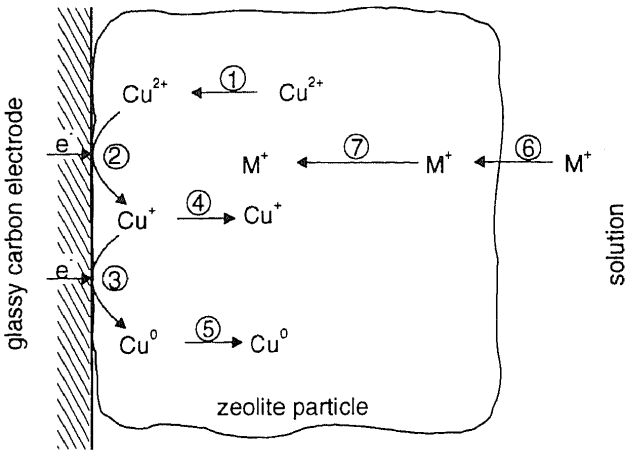

Fig. 12. Possible rate-limiting steps in the electrochemical reduction of Cu^{2+} at the Cu^{2+}-Y-modified glassy carbon electrode in chloride electrolyte: (1) diffusion of Cu^{2+} ions from the bulk of the zeolite to the surface; (2) reduction of Cu^{2+} to Cu^+; (3) reduction of Cu^+ to Cu^0; (4) diffusion of Cu^+ into the bulk of the zeolite; (5) diffusion of Cu^0 into the bulk of the zeolite; (6) movement M^+ into the zeolite to maintain charge neutrality; (7) diffusion of M^+ within the zeolite.

respect to the glassy carbon electrode. The potential of peak D is nearly the same as that of D_{GC}.

3.8. Model of the electrochemical reduction of Cu^{2+}

A model for the electrochemical reduction of Cu^{2+} at the Cu^{2+}-Y-modified electrode in chloride electrolyte, based on our results, is proposed in Fig. 12. Step 1 is the diffusion of Cu^{2+} ions within the zeolite, steps 2 and 3 are the reduction of Cu^{2+} and Cu^+ at the zeolite side of the three-component interface, steps 4 and 5 are the diffusion of Cu^+ and Cu^0 into the zeolite, step 6 is the movement of the electrolyte cation M^+ into the zeolite to maintain charge neutrality in the zeolite and step 7 is the diffusion of M^+ ions

TABLE 5. Peak potentials, apparent formal potentials and difference of peak potential differences [a]

MCl (0.1 M)	$Cu_{10.6}Na_{34.8}$-Y-modified electrode				Glassy carbon electrode		
	E_{pc}/V(SCE)	E_{pa}/V(SCE)	$\Delta E_{p(C\text{-}A)}$/V(SCE)	$E^{\circ}_{II/I(z)}$/V(SCE)	E_{pc}/V(SCE)	E_{pa}/V(SCE)	$E^{\circ}_{II/I(s)}$/V(SCE)
NaCl	−0.044(A)	0.072(C)	0.116	0.014	0.050(A_{GC})	0.145(C_{GC})	0.098
	−0.254(B)	0.011(D)			−0.287(B_{GC})	0.006(D_{GC})	
KCl	−0.003	0.109	0.112	0.053	0.051	0.145	0.098
	−0.255	−0.007			−0.289	−0.002	
CsCl	0.001	0.093	0.092	0.047	0.051	0.143	0.097
	−0.281	−0.029			−0.289	−0.025	
LiCl	−0.105	0.066	0.171	−0.020	0.059	0.141	0.100
	−0.255	0.016			−0.294	−0.004	

[a] The data are obtained from Figs. 10 and 11: A, B, C, D, A_{GC}, B_{GC}, C_{GC} and D_{GC} represent the peaks as shown in Figs. 10 and 11; E_{pc} and E_{pa} represent the cathodic and anodic peak potentials respectively. $\Delta E_{p(C\text{-}A)}$ is the difference between the potentials of peaks C and A; $E^{\circ}_{II/I}$ is the apparent formal potential of Cu^{2+}/Cu^+ which is calculated by $(E_{p(C)} + E_{p(A)})/2$ and $(E_{p(C_{GC})} + E_{p(A_{GC})})/2$.

within the zeolite. In nitrate electrolyte, steps 2 and 3 are replaced by a single step in which Cu^{2+} is directly reduced to Cu^0 via a two-electron process. Any of the steps shown in the diagram may be rate limiting, giving a characteristic signature to the electrode reaction.

3.9. The rate-limiting step in the reduction of Cu^{2+} to Cu^+

Table 4 shows that the peak current $I_{p(A)}$ of A in Figs. 10 and 11 is strongly affected by the electrolyte cation in the chloride electrolyte. The order of decreasing peak current $I_{p(A)}$ of A is

$$Na^+ > K^+ > Cs^+ > Li^+ \quad (4)$$

This observation indicates clearly that the electrode process depends on the nature of M^+ and therefore is determined by steps 6 and 7. As discussed above, the migration of ions into the zeolite is faster than the diffusion of ions within the zeolite. It can be concluded that the electrode process of the electrochemical reduction of Cu^{2+} ions at the $Cu_{10.6}Na_{34.8}$-Y-modified electrode is controlled by the diffusion of the electrolyte cation within the Y zeolite, i.e. step 7 in Fig. 12 is a rate-limiting process.

3.10. Influence of the leaching of Cu^{2+} out of the zeolite

If the diffusion of the electrolyte cations inside the zeolite is a rate-limiting process, then the order of decreasing current $I_{p(A)}$ of A should be $Cs^+ > K^+ > Na^+ > Li^+$ according to (3a) or (3b). However, this is not in agreement with observation (4). The peak current is determined not only by the diffusion but also by the concentration. When a voltammetry experiment with an electroactive species zeolite-modified electrode is carried out in electrolyte solution, the loss of the electroactive species from the zeolite to the solution by ion exchange cannot be avoided except when the electroactive species is too large to escape from the zeolite cage. Therefore the actual concentration of the electroactive species in the zeolite during the measurement is smaller than its initial concentration in the zeolite (before inserting the electrode into the solution). Sequence (2) indicates that the sequence of the rate of loss of Cu^{2+} ions from the Y zeolite by ion exchange in 0.1 M MCl aqueous solution is $Cs^+ \gg K^+ > Na^+ > Li^+$ in the case of the $Cu_{10.6}Na_{34.8}$-Y-modified electrode. Thus the actual concentration of Cu^{2+} ions in the Y zeolite during the measurements is smaller than the initial concentration and is expected to be in the following order:

$$c'_{Cs} \ll c'_K < c'_{Na} < c'_{Li} < c^* \quad (5)$$

where c' and c^* are the actual and initial concentrations respectively. Sequence (4) is observed as a result of (3) or (5). When an experiment is carried out by inserting an electroactive species zeolite-modified electrode into an electrolyte solution, losses by ion exchange must be considered.

3.11. Diffusion of the Cu^+ ions into the zeolite

As shown in Fig. 11, the current of peak C is much smaller than that of A in NaCl, KCl and CsCl electrolytes, but $I_{p(A)}$ and $I_{p(C)}$ are nearly equal in LiCl. In order to measure $I_{p(C)}$ accurately, the voltammetric experiments have been carried out by holding the potential at the switching potential for 6 s to make the current fall to the baseline. The $I_{p(C)}$ values measured in the different electrolytes are reported in Table 4. The ratio $I_{p(C)}/I_{p(A)}$ of the currents increases in the following order:

$$K^+ < Na^+ < Cs^+ < Li^+ \quad (6)$$

During the negative scan the concentration of the Cu^+ ions produced at the three-component interface increases. Some of them diffuse so deep into the interior of the zeolite (far away from the contact area) that they cannot be reoxidized during the positive scan. The amount of this part of Cu^+ depends on the concentration of Cu^+ ions produced at the interface, their diffusion rate and the electrolyte cations in the Y zeolite. The higher the concentration of the Cu^+ ions produced and the faster their diffusion within the Y zeolite, the larger is the amount of Cu^+ ions which cannot be reoxidized. If we assume that the diffusion of the Cu^+ in the Y zeolite is faster than that of the electrolyte cations, then the amount of Cu^+ which moves deep into the zeolite during the scan is determined by the diffusion rate of the electrolyte cations within the zeolite. As a result, the amount of this Cu^+ decreases in the order

$$Cs^+ > K^+ > Na^+ > Li^+ \quad (7)$$

according to sequence (3a) or (3b), for a constant Cu^+ concentration. In addition, the charge under peak A in 0.1 M CsCl is much smaller than that in 0.1 M NaCl and KCl as shown in Table 4, which means that the amount of Cu^+ ions produced in 0.1 M CsCl is less than that in 0.1 M NaCl and KCl. Combining the effects of diffusion of the electrolyte cations and the amount of Cu^+ ions produced (i.e. the concentration of Cu^+ ions at the interface) results in sequence (6). We conclude that the observed deviation of the ratio $I_{p(C)}/I_{p(A)}$ from unity is caused by the diffusion of some of the Cu^+ ions produced deep into the Y zeolite. This also explains the observed values of Q_B/Q_A and $I_{p(B)}/I_{p(A)}$ (Table 4).

3.12. Conductivity of the zeolite layer

No $I(R_s + R_z)$ compensation has been made in any of our experiments. R_s and R_z are the resistances of

the electrolyte solution and the zeolite-modified layer respectively. In the case of the unmodified glassy carbon electrode, the differences ΔE_p in the peak potentials are almost the same in the different electrolytes (see Table 5). This indicates that IR_s is little influenced by the electrolyte cations. The differences $\Delta E_{p(C-A)}$ between the potentials of the peaks C and A are larger for the $Cu_{10.6}Na_{34.8}$-Y-modified electrode than those observed at the unmodified glassy carbon electrode and depend on the electrolyte cations. $\Delta E_{p(C-A)}$ decreases in the order

$$Li^+ > Na^+ > K^+ > Cs^+ \quad (8)$$

The zeolite can be considered as a solid electrolyte and its conductivity depends on the mobility of its cations. The larger their mobility, the larger is the conductivity of the zeolite. Based on the sequence (3a) or (3b), the conductivity of the Y zeolite layer in the electrolyte solutions used decreases as follows:

$$Cs^+ > K^+ > Na^+ > Li^+ \quad (9)$$

However, the resistance R_z decreases in the order

$$Li^+ > Na^+ > K^+ > Cs^+ \quad (10)$$

which is in good agreement with sequence (8) and indicates that the increase in $\Delta E_{p(C-A)}$ for the zeolite-modified electrodes is mainly caused by the uncompensated IR_z.

In addition, Table 5 shows that the ΔE_p in 0.1 M CsCl solution is the same for both the modified and the unmodified electrodes. From this and sequence (3a) or (3b), we conclude that the mobilities of Cu^{2+} and Cs^+ in the supercages of the Y zeolite are the same and are the same as in water.

3.13. Semi-infinite linear diffusion in the zeolite Y layer?

Table 4 shows that the charge under peak A depends on the electrolyte cations and decreases in the order

$$Na^+ > K^+ > Cs^+ > Li^+ \quad (11)$$

Regardless of any losses of Cu^{2+} into the solution by ion exchange, 56%, 45%, 35% and 35% of the initial Cu^{2+} ions were reduced in NaCl, KCl, CsCl and LiCl respectively. Since the loss of Cu^{2+} ions to the solution by ion exchange cannot be avoided in these experiments, the actual percentages must be larger than the calculated values. We conclude that the semi-infinite liner diffusion condition [26] does not apply to the $Cu_{10.6}Na_{34.8}$-Y-modified electrodes.

3.14. Shift of the apparent formal potential of Cu^{2+}/Cu^+

The apparent formal potential of Cu^{2+}/Cu^+ for the $Cu_{10.6}Na_{34.8}$-Y-modified electrodes shifts in the negative direction with respect to the glassy carbon electrode, as shown in Table 5. The same behaviour has been reported for Nafion®-modified electrodes [27] and clay-modified electrodes [28]. The shift in the apparent formal potential of Cu^{2+}/Cu^+ for Cu^{2+}-Y-modified electrodes can be described by

$$\Delta E^{\alpha} = E^{\alpha}_{II/I(z)} - E^{\alpha}_{II/I(s)} = \frac{RT}{F} \ln \frac{K_I[M^+]_{(s)}}{K_{II}[M^+]_{(z)}} \quad (12)$$

where $E^{\alpha}_{II/I(z)}$ is the apparent formal potential of Cu^{2+}/Cu^+ within the zeolite layer, $E^{\alpha}_{II/I(s)}$ is the formal potential of Cu^{2+}/Cu^+ measured at the unmodified electrode, K_I and K_{II} are the selectivity coefficients for the ion exchange reactions of the Cu^{2+} and Cu^+ with the ion exchange sites in the zeolite respectively, and $[M^+]_{(z)}$ and $[M^+]_{(s)}$ are the concentrations of M^+ in the zeolite layer and solution respectively. Equation (12) indicates that the shift of the apparent formal potential of Cu^{2+}/Cu^+ for the Cu^{2+} exchanged Y zeolite modified electrode depends on the selectivity coefficients K_{II} and K_I and the concentrations of M^+ in the solution and in the zeolite Y layer. Strictly speaking, eqn. (12) is only suitable for the case in which the co-cation in the zeolite is the same as the electrolyte cation in the solution. In our experiments, the concentration $[M^+]_{(s)}$ of the electrolyte cation in the solution was 0.1 M and the temperature was 293 K. If the effect of the co-cation is negligible, then eqn. (12) can be written

$$\Delta E^{\alpha}/V = 0.058 \log(K_I/K_{II}[M^+]_{(z)}) - 0.058 \quad (13)$$

This equation indicates that $E^{\alpha}_{II/I(z)}$ deviates from $E^{\alpha}_{II/I(s)}$ and that the extent of the shift depends on the nature of the electrolyte cation, which is in agreement with the experimental observation.

4. Conclusions

The monograin zeolite-modified glassy carbon electrodes prepared by the method described in this paper are mechanically stable, and voltammetric experiments with these electrodes show good reproducibility.

Cu^{2+} ions in A zeolites are 'electrochemically silent' in the potential range from 0.5 to −0.8 V/SCE in sharp contrast with the Cu^{2+} ions in the Y zeolite. This is probably due to relatively strong coordination of Cu^{2+} ions to the framework of the A zeolite, causing slow diffusion in its cages and channels, and is in agreement with the fact that A zeolites do not support high Cu^{2+} loading.

The relative diffusion rates of the alkali and Cu^{2+} cations in the Y zeolite are $Cu^{2+} \approx Cs^+ > K^+ > Na^+ > Li^+$, and the mobilities of Cs^+ and Cu^{2+} in water and in the zeolite Y are nearly identical.

The experiments show that, for thick-layer zeolite-modified electrodes, only the Cu^{2+} ions in the first layer take part in the electrode process. The following layers play a role only decreasing the loss of Cu^{2+} ions of the first layer.

Significant differences between the cyclic voltammetric behaviour of the $Cu_{10.6}Na_{34.8}$-Y-modified electrodes and Cu^{2+} ions at the unmodified glassy carbon electrode are observed. They clearly indicate that the electrochemical behaviour of the $Cu_{10.6}Na_{34.8}$-Y-modified electrodes cannot be explained by a process in which the Cu^{2+} ions are ion exchanged into the solution, diffuse to the uncovered part of the surface of the glassy carbon electrode and then are electrochemically reduced. The considerable influence of the electrolyte anions on the electrode process at the $Cu_{10.6}Na_{34.8}$-Y-modified electrodes indicates that the electrochemical reduction of Cu^{2+} ions at the $Cu_{10.6}Na_{34.8}$-Y-modified electrodes does not occur within the bulk of the zeolite. We conclude that the electrochemical processes occur at the zeolite side of the glassy carbon/solution/zeolite interface as explained in Fig. 12. We call this kind of electrode process an intrazeolite ion transport mechanism to distinguish it from another intrazeolite process which has been found in silver A-zeolite-modified electrodes [14,17]. In the electrochemical reduction process of Cu^{2+} to Cu^{+}, the diffusion of the electrolyte cation within the Y zeolite is a rate-limiting process. The experiments show that the semi-infinite linear diffusion model is not suitable for the electrode process at the Cu^{2+} zeolite-modified electrode. The apparent formal potential of Cu^{2+}/Cu^{+} in the zeolite shifts from that of Cu^{2+}/Cu^{+} in the solution and depends on the nature of the electrolyte cations. Also, the conductivity of the Y-zeolite-modified layer depends on the electrolyte cations and decreases in the order $Cs^{+} > K^{+} > Na^{+} > Li^{+}$.

Acknowledgements

We would like to thank Professor R. Giovanoli and his staff at the Electron Microscopy Laboratory, University of Berne, for invaluable SEM and X-ray diffraction measurements. This research is part of project NF 20-34042.92, financed by the Schweizerische Nationalfonds zur Föderung der wissenschaftlichen Forschung and project BEW-EPA 217.307, financed by the Schweizerische Bundesamt für Energiewirtschaft.

References

1 D.R. Rolison, Chem. Rev., 90 (1990) 867.
2 D.R. Rolison, R.J. Nowak, T.A. Welsh and C.G. Murray, Talanta, 38 (1991) 27.
3 G.A. Ozin, A. Kuperman and A. Stein, Angew. Chem. Int. Ed. Engl., 28 (1989) 359.
4 B. de Vismes, F. Bedioui and J. Devynck, J. Electroanal. Chem., 187 (1985) 197.
5 H.A. Gemborys and B.R. Shaw, J. Electroanal. Chem., 208 (1986) 95.
6 Z. Li and T.E. Mallouk, J. Phys. Chem., 91 (1987) 643.
7 B.R. Shaw, K.E. Creasy, C.J. Lanczycki, J.A. Sargeant and M. Tirhado, J. Electrochem. Soc., 135 (1988) 869.
8 M.D. Baker, C. Senaratne and J. Zhang, J. Chem. Soc. Faraday Trans., 88 (1992) 3187.
9 K.E. Creasy and B.R. Shaw, Electrochim. Acta, 33 (1988) 551.
10 B.R. Shaw and K.E. Creasy, J. Electroanal. Chem., 243 (1988) 209.
11 M.D. Baker and J. Zhang, J. Phys. Chem., 94 (1990) 8703.
12 F. Bedioui, E. De Boysson, J. Devynck and K.J. Balkus Jr., J. Electroanal. Chem., 315 (1991) 313.
13 J. Wang and T. Martinez, Anal. Chim. Acta, 207 (1988) 95.
14 J. Li and G. Calzaferri, J. Chem. Soc. Chem. Commun., (1993) 1430.
15 N. El Murr, M. Kerkeni, A. Sellami and Y. Ben Taarit, J. Electroanal. Chem., 246 (1988) 461.
16 M.D. Baker and C. Senaratne, Anal. Chem., 64 (1992) 697.
17 J. Li, Dissertation, University of Berne, 1993.
18 M.W. Anderson and L. Kevan, J. Phys. Chem., 91 (1987) 1850.
19 J.S. Yu and L. Kevan, J. Phys. Chem., 94 (1990) 7612.
20 D.W. Breck, Zeolite Molecular Sieves, Wiley, New York, 1974.
21 G. Calzaferri, R. Giovanoli, I. Kamber, V. Shklover and R. Nesper, Res. Chem. Intermed., 19 (1993) 31.
22 F. Bedioui, E. De Boysson, J. Devynck and K.J. Balkus Jr, J. Chem. Soc. Faraday Trans., 87 (1991) 3831.
23 L. Gaillon, N. Sajot, F. Bedioui and J. Devynck, J. Electroanal. Chem., 345 (1993) 157.
24 R.M. Barrer and A.J. Walker, Trans. Faraday Soc., 60 (1964) 171.
25 R.M. Barrer and W.M. Meier, J. Chem. Soc., (1958) 299.
26 A.J. Bard and L.R. Faulkner, Electrochemical Methods, Wiley, New York, 1980, p. 218.
27 R. Naegeli, J. Redepenning and F.C. Anson, J. Phys. Chem., 90 (1986) 6227.
28 A. Fitch, J. Electroanal. Chem., 284 (1990) 237.